Doublecortin Is a Developmentally Regulated, Microtubule-Associated Protein Expressed in Migrating and Differentiating Neurons

Fiona Francis,*‖ Annette Koulakoff,†
Dominique Boucher,† Philippe Chafey,*
Bruce Schaar,‡ Marie-Claude Vinet,*
Gaëlle Friocourt,* Nathalie McDonnell,*
Orly Reiner,§ Axel Kahn,* Susan K. McConnell,‡
Yoheved Berwald-Netter,† Philippe Denoulet,†
and Jamel Chelly*
*U129 de l'INSERM
Institut Cochin de Génétique Moléculaire
24, rue du Faubourg Saint Jacques
75014 Paris
†Laboratoire de Biochimie Cellulaire
CNRS UPR 9065
Collège de France
11, Place M. Berthelot
75005 Paris
France
‡Department of Biological Sciences
Stanford University
Stanford, California 94305
§Department of Molecular Genetics
The Weizmann Institute of Science
76100 Rehovot
Israel

Summary

Recently, we and others reported that the *doublecortin* gene is responsible for X-linked lissencephaly and subcortical laminar heterotopia. Here, we show that Doublecortin is expressed in the brain throughout the period of corticogenesis in migrating and differentiating neurons. Immunohistochemical studies show its localization in the soma and leading processes of tangentially migrating neurons, and a strong axonal labeling is observed in differentiating neurons. In cultured neurons, Doublecortin expression is highest in the distal parts of developing processes. We demonstrate by sedimentation and microscopy studies that Doublecortin is associated with microtubules (MTs) and postulate that it is a novel MAP. Our data suggest that the cortical dysgeneses associated with the loss of Doublecortin function might result from abnormal cytoskeletal dynamics in neuronal cell development.

Introduction

During development of the mammalian brain, neurons migrate long distances to form the complex laminar structures of the cerebral cortex (reviewed by McConnell, 1995). Neocortical neurons arise in the ventricular neuroepithelium, which contains proliferating precursor cells. Postmitotic neurons exit the neuroepithelium in waves, the earliest to arrive in the cortical plate settle in the deeper layers, while later born neurons cross through these layers to successively reach regions closer to the cerebral surface (reviewed by McConnell, 1995; Caviness et al., 1997). In this way, a six-layered neocortex develops. Migrating neurons mainly travel in association with radially extending glial fibres (Rakic, 1971; Luskin et al., 1988); however, tangential and chain migration have also been observed in some brain regions (Luskin, 1993; Tan and Breen, 1993; O'Rourke et al., 1995; Lois et al., 1996). Many questions still remain concerning the corticogenesis process: the signals that determine the timing of cells leaving the proliferative pool, which ultimately affects their laminar fate (Frantz and McConnell, 1996), the mechanism and direction of cell locomotion, and the recognition of the final destination.

Lissencephaly is a cortical malformation disorder associated with severe mental retardation and epilepsy (Harding, 1996), which exists as an X-linked disease (X-LIS) caused by mutations in the *doublecortin* gene (des Portes et al., 1998a; Gleeson et al., 1998). Another related disorder is Miller Dieker syndrome consisting of lissencephaly with characteristic facial abnormalities (Dobyns et al., 1991), which is associated with the loss of function of the *LIS1* gene product (Reiner et al., 1993; Hattori et al., 1994). Patients with lissencephaly have a thickened disorganized cortex, lacking the characteristic laminar pattern, and the surface of the brain is smooth without the gyri or folds found in normal individuals. X-LIS is often associated within the same pedigree with a second cortical dysgenesis disorder, subcortical laminar heterotopia (SCLH, Pinard et al., 1994), which mainly affects females, and is characterized by an apparently true cortex, but with a heterotopic layer of misplaced neurons. Mutations in the *doublecortin* gene account for most cases of SCLH (des Portes et al., 1998b). Both X-LIS and SCLH are believed to be disorders of neuronal migration; however, the function of Doublecortin and the pathophysiological mechanisms that result from its deficit remain unknown.

Several other genes have been isolated that, when disrupted, cause neuronal migration disorders in mice. One of them encodes Reelin, an extracellular matrix protein expressed by the Cajal-Retzius cells of the marginal zone (D'Arcangelo et al., 1995; Hirotsune et al., 1995), which is mutated in the *reeler* mouse. Since Reelin is a secreted protein, its mode of action may be as a guidance molecule or stop signal for migrating neurons (reviewed by Pearlman et al., 1998). Mdab1, a protein involved in signaling, is mutated in *scrambler* and *yotari* mice, which have a very similar phenotype to *reeler* (Howell, et al., 1997; Sheldon et al., 1997; Ware et al., 1997). Two other signaling genes implicated in neuronal migration are cyclin-dependent kinase 5 (Cdk 5), a brain-specific kinase, and its neuronal specific activator p35 (Ohshima et al., 1996; Chae et al., 1997). Multiple molecular mechanisms are thus implicated in the formation of the cortex.

Major cytoskeletal changes are required in active migration (Rivas and Hatten, 1995; Rakic et al., 1996): the

‖To whom correspondence should be addressed (e-mail: ffrancis@infobiogen.fr).

neuronal cell extends a leading process toward the target destination, followed by a translocation of the nucleus and of cytoplasmic components (Rakic, 1971; Komuro and Rakic, 1995). Axonal elongation is similarly dependent upon cytoskeletal dynamics (reviewed by Gordon-Weeks, 1991; Tanaka and Sabry, 1995). Identifying the molecules that participate in these cytoskeletal events is thus of considerable interest. It is clear that both microtubules (MTs) and actin filaments are important: both are present in leading and axonal processes, and the nucleus is surrounded by a MT network underlying a rim of actin filaments (Rivas and Hatten, 1995). Interestingly, LIS1 was shown to interact with tubulin and to have an effect on MT dynamics (Sapir et al., 1997). Other recent data suggest that Cdk5 and p35 influence the reorganization of the actin cytoskeleton (Nikolic et al., 1998).

In the present study, we have begun to explore the role of Doublecortin in neuronal development. We show that Doublecortin is a developmentally regulated, neuron-specific phosphoprotein, localized in cell bodies and the leading processes of migrating neurons and the axons of differentiating neurons. Our ex vivo and in vitro data show that Doublecortin is associated with MTs, suggesting that it is involved in the regulation of MT dynamics.

Results

Characterization of Polyclonal Antibodies Specific to Doublecortin

Two different polyclonal antibody preparations, one directed against synthetic peptides (anti-Doublecortin pep) and the other against an N-terminal fusion protein (anti-N-term), were used to detect Doublecortin. As shown in Figure 1A, anti-Doublecortin pep antibodies reveal in human fetal brain a band of approximately 40 kDa, which is the predicted molecular weight of Doublecortin. In mouse extracts from E12.5 to newborn, a band of the same size and higher molecular weight bands were detected (the upper band is a doublet as shown in Figure 1B). These bands were absent at E10.5 and in the adult indicating that Doublecortin expression is developmentally regulated. The bands detected are likely to be specific since preincubation of antisera with the synthetic peptides completely blocked the detection of all bands, and preimmune sera gave no signal on the Western blots. The presence of several bands (Figure 1B) suggests that Doublecortin may be posttranslationally modified. Treatment of neonatal mouse brain protein extracts with alkaline phosphatase led to the disappearance of the upper doublet (Figure 1B). Addition of sodium pyrophosphate, a phosphatase inhibitor, prior to the phosphatase, resulted in the detection of all bands. Hence, Doublecortin exists in a phosphorylated form, and indeed several potential phosphorylation sites were previously predicted (des Portes et al., 1998a; Gleeson et al., 1998).

In order to explore Doublecortin expression in maturing neurons, cell extracts from primary cultures grown for 2, 6, 9, 12, 18, 24, and 30 days (Berwald-Netter et al., 1981) were screened with Doublecortin antibodies,
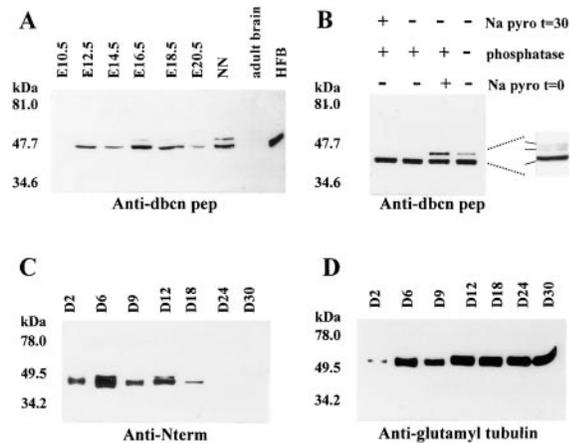
Figure 1. Doublecortin Antibodies Detect a 40 kDa Phosphoprotein in Developing Mouse and Human Tissues and in Neuronal Cultures

(A) Anti-Doublecortin pep antibodies (Anti-dbcn pep) were used to probe Western blots of extracts from total mouse embryo at day 10.5–14.5, fetal mouse head extracts from embryonic day 16.5–20.5, mouse brain extracts from neonates (NN), and adult mice, and human fetal brain extracts (HFB). Expanded region (B) shows the three bands detected.

(B) Anti-Doublecortin pep antibodies were used to probe extracts from mouse neonatal brain that had been treated with alkaline phosphatase. Lane 1, treatment with 30 U of alkaline phosphatase for 30 min at 30°C, followed by the addition of 10 mM sodium pyrophosphate (inhibitor); lane 2, treatment with alkaline phosphatase alone; lane 3, treatment with alkaline phosphatase in the presence of the inhibitor; and lane 4, control sample incubated for 30 min at 30°C. In lanes 1 and 2, the upper doublet of Doublecortin bands are susceptible to alkaline phosphatase treatment.

(C) Anti-N-term antibodies were used to probe extracts from primary cultures of mouse brain neurons grown for 2, 6, 9, 12, 18, 24, and 30 days. Doublecortin expression diminishes with increasing time in culture.

(D) The same extracts as in (C) were screened with antibody, GT335 specific for glutamylated tubulin (Anti-glutamyl tubulin).

which revealed an expression in young neurons that diminishes with neuronal maturation and is undetectable in extracts from 24- and 30-day-old cultures (Figure 1C). Phosphorylated forms of Doublecortin were observed as noted previously with the mouse tissue extracts. An antibody, GT335, directed at glutamylated tubulin was used in parallel against the same extracts: a band of 50 kDa (corresponding to $\alpha\beta$-tubulin) was detected in all samples (Figure 1D), with a slight increase in expression with time in culture, as expected during neuronal maturation (Audebert et al., 1994). Hence, Doublecortin is only detected in young differentiating neurons in culture. Western blot analysis was also performed on cultured glial cells obtained from newborn mice, and no Doublecortin was detected, confirming that its expression is specific to neurons (data shown in Figure 5).

Temporal and Spatial Expression Patterns of Doublecortin

A series of RNA in situ hybridizations and immunohistochemical studies were performed on mouse and rat embryo sections of different stages in order to define more
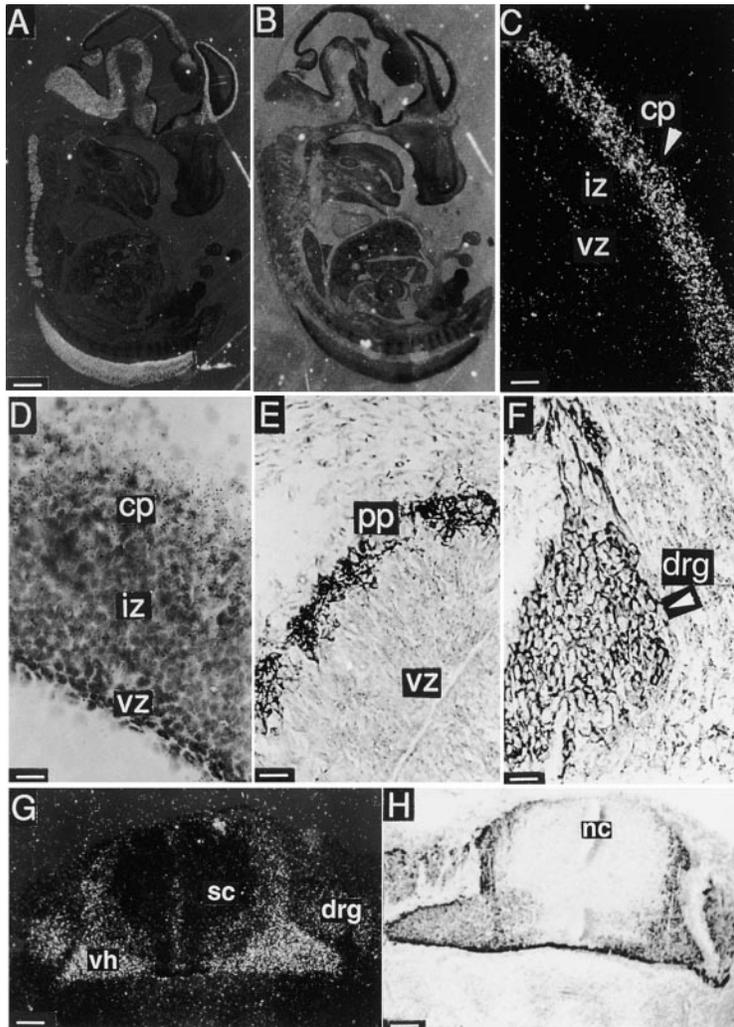
Figure 2. Localization of Doublecortin mRNA and Protein in Mouse Embryonic Sections

(A and B) Sagittal sections from E14.5 mouse embryos viewed in dark field. (A), the anti-sense probe; (B), the sense probe.

(C and D) Higher magnifications of the ventricular wall ([C], dark field; [D], bright field); note intense labeling in the cortical plate/marginal zone regions. In bright field, this labeling is shown as deposited small black grains. cp, cortical plate; iz, intermediate zone; vz, ventricular zone.

(E) Immunodetection of an area from the ventricle wall from a sagittal section of E11.5 mouse. Strong Doublecortin labeling is observed in the preplate region (pp).

(F) Immunostaining of a dorsal root ganglion (drg) taken from the same embryo section as (E). Note localization of Doublecortin in neuronal somata and fibers.

(G and H) Developing spinal cord (sc) and ganglia (drg) at E11.5 (G) in situ RNA hybridization viewed at dark field; note intense labeling of the ventral horn region (vh). (H) A corresponding region in a serial section where Doublecortin protein is detected with anti-N-term antibody. nc, neural canal.

Scale bars are as follows: (A and B), 550 μm; (C), 25 μm; (D), 8 μm; (E and F), 15 μm; (G and H), 50 μm.

accurately the temporal and spatial profile of Doublecortin expression. Observations were made initially at low magnification in order to determine the regional distribution. Using a 5' UTR RNA probe, no specific signals were observed at mouse embryonic day 9.5, whereas at day 10.5 very weak signals were visible in the neuroepithelium. Sections of mouse embryos taken at ages 11.5, 12.5, 14.5, and 16.5 show a noticeably stronger labeling in the telencephalon, diencephalon, and mesencephalon, in the olfactory lobes, the developing cerebellum, the brain stem, the spinal cord, and the dorsal root ganglia (Figure 2A). In brain sections from 18 day embryos and neonates, labeling was observed in all brain regions examined.

Interestingly, in the developing cerebral cortex, very little label was seen in the ventricular and intermediate zones, but instead a high deposition of silver grains was observed in the cells of the developing preplate or cortical plate/marginal zone regions (Figures 2C and 2D). The distribution of Doublecortin examined by immunohistochemistry with the two antisera was found to be very similar to the *doublecortin* transcript. In Figure 2E, high magnification of a section through the ventricular

wall at E11.5 shows staining of neurons in the preplate, and Doublecortin is detectable in the cell somata as well as the fibers. This localization is also visible in Figure 2F in dorsal root ganglia neurons. In sections of the spinal cord at E11.5 (Figures 2G and 2H), Doublecortin is predominantly expressed in the ventral horn region, suggesting that it is abundant in long projecting neurons.

Double-labeling experiments were performed in rat brain sections: Doublecortin was compared to β III tubulin, which has been previously shown to be present in migrating and differentiating, postmitotic neurons in the developing cortex (Lee et al., 1990). In general, Doublecortin antibodies decorated the same cells as those labeled for β III tubulin, and labeling was observed at all embryonic stages examined (E14, E15, E16, E18, and E19). Staining of E14 brain sections (approximately equivalent to mouse stage E12) showed strong Doublecortin expression in the preplate region (Figures 3A–3C). In sections from older embryos (Figures 3D–3G), there was extensive labeling in the cortical plate and intermediate zone regions. Doublecortin labeling in the intermediate zone was verified in comparison with Syto 11 staining of cell nuclei, which are particularly dense in the ventricular
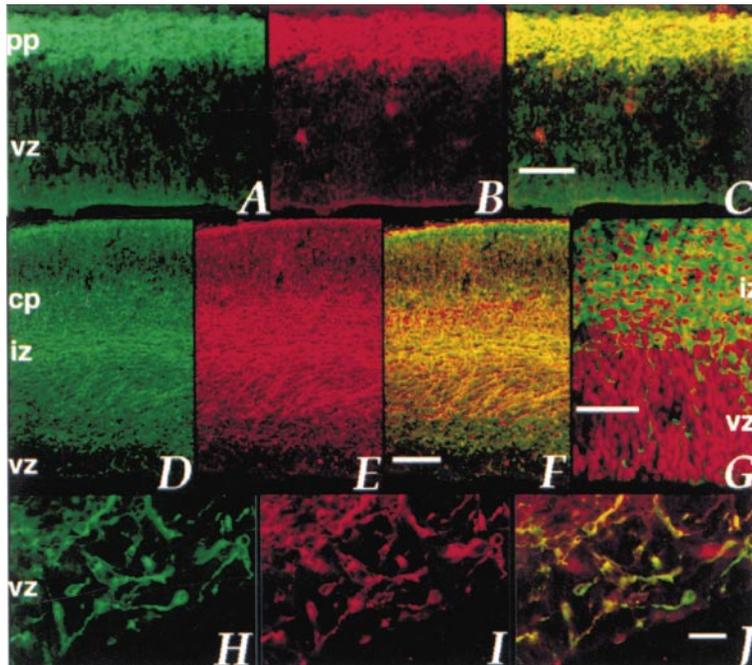
Figure 3. Doublecortin and β III Tubulin Are Coexpressed in the Developing Rat Brain

(A–F) Double immunostained sections of fetal rat neocortex at E14 (A–C) and E18 (D–F), stained for Doublecortin using anti-N-term ([A, D, and H], pseudocolored green) and β III tubulin using TuJI ([B, E, and I], pseudocolored red).

(G) E16 section where DNA staining is red (Syto-11 labeling) and Doublecortin is green.

(H–J) Higher magnification of tangentially migrating neurons in E18 ventricular zone. Merged images of Doublecortin and TuJ1 (C, F, and J) show extensive overlap of expression.

Scale bars: (C), 75 μm; (F), 50 μm; (G), 25 μm; (J), 25 μm.

zone (Figure 3G). A strong labeling of axons (giving rise to a striped appearance in Figures 3D–3F) makes it difficult to determine if radially migrating neurons are also labeled. Higher magnification nevertheless revealed the presence of Doublecortin in tangentially migrating neurons in the ventricular zone (Figures 3H–3J) coexpressing β III tubulin. In these migrating cells, Doublecortin is clearly distributed in the leading processes and cell bodies.

Expression of Doublecortin in Primary Cultures of Brain Neurons

The use of neuronal cell cultures enabled us to further investigate the subcellular distribution of Doublecortin and to assess its evolution in the course of neuronal maturation. Cells were doubly labeled with anti-Doublecortin pep and antibodies directed against cytoskeletal proteins (Figure 4). Interestingly, Doublecortin antibodies revealed a nonhomogeneous distribution of the protein with a bright staining in the distal parts of many neurites, and much fainter labeling observed elsewhere (Figure 4A). In contrast, the anti-α-tubulin antibodies gave a relatively even labeling of neuronal somata and fibers (Figure 4B). Doublecortin expression was followed in neurons during their maturation in culture: the particular distribution in the distal parts of neurites was already present in immature neurons grown for only 16 hr and persisted throughout the time period of Doublecortin expression indicated by the Western blot results. Neurons grown for 21 to 30 days in culture, although strongly labeled with anti-tubulin antibodies, were not labeled with anti-Doublecortin pep antibodies, indicating a large reduction of expression. The expression of Doublecortin and its distribution were not modified when neurons were grown on a matrix of glial cells. The staining was also assessed with the anti-N-term antibody, and its concentration was varied to help assess the localization

of Doublecortin. Indeed, at high concentrations, the anti-N-term antibody decorates neuronal somata and the whole-length of the neurites; however, their distal parts were most strongly labeled, confirming the enrichment of Doublecortin in these regions.

We further examined the extent of the Doublecortin staining with respect to the growth cones that were present at the ends of some neurites. Staining for actin revealed the entire growth cone, of which Doublecortin was found in only the proximal part (Figure 4C). It was not possible to distinguish between dendrites and axons in the young cultured neurons: MAP2, which is known to be abundant in dendrites in vivo (Bernhardt and Matus, 1984), was detected in almost all neurites. Interestingly, double labeling with anti-MAP2 and anti-Doublecortin pep shows bright MAP2 staining along the length of the neurite tapering off at approximately the same region where Doublecortin becomes abundant (Figures 4E and 4F).

Association with MTs

The subcellular distribution of Doublecortin and the fact that LIS1 was shown to interact with tubulin (Sapir et al., 1997) led us to hypothesize that Doublecortin may also be associated with MTs. Neuronal cultures were treated with nocodazole and taxol in order to test, respectively, the effect of the depolymerization and hyperpolymerization of MTs on the distribution of Doublecortin. As shown by immunocytofluorescence, nocodazole treatment leads to a redistribution of Doublecortin labeling in parallel with that of tubulin: Doublecortin staining becomes diffuse and uniformly distributed in the neuron (Figures 4G and 4H). Treatment of the cells with cytochalasin B, which disrupts the actin cytoskeleton, showed no differences in the distribution of the protein compared to control cells (data not shown). Hence, the enrichment of Doublecortin in the distal regions of the neurites is dependent upon MT organization. There was
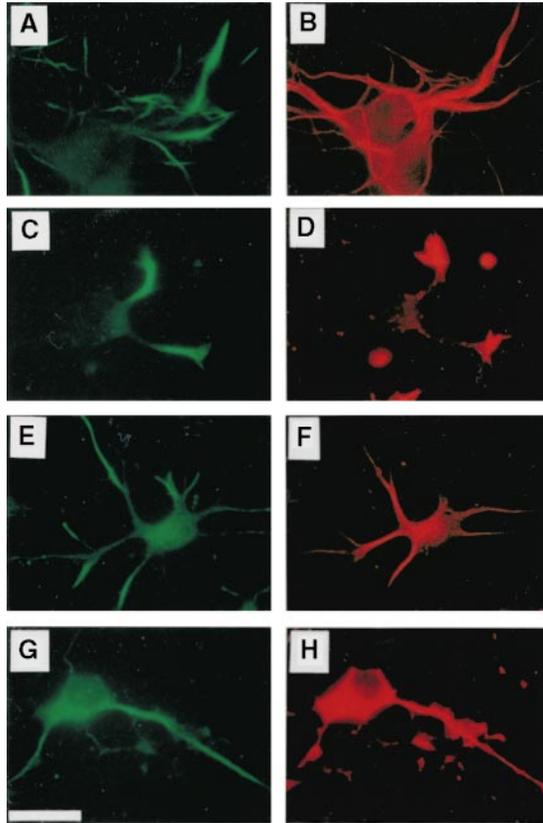
Figure 4. Subcellular Localization of Doublecortin in Brain Neurons in Culture, Compared to Tubulin, Actin, or MAP2

(A and B) Neurons grown for 6 days in culture were doubly labeled with anti-Doublecortin pep (A) and anti-α-tubulin (B).
(C and D) Details of growth cones in neurons grown 2 days in culture doubly stained with anti-Doublecortin pep (C) and anti-actin (D).
(E and F) Neurons (6 days) were doubly labeled with anti-Doublecortin pep (E) and anti-MAP2 (F).
(G and H) The effect of microtubule disruption by nocodazole treatment shown by double labeling with anti-Doublecortin pep (G) and anti-α-tubulin (H). The scale bar corresponds to 25 μm.
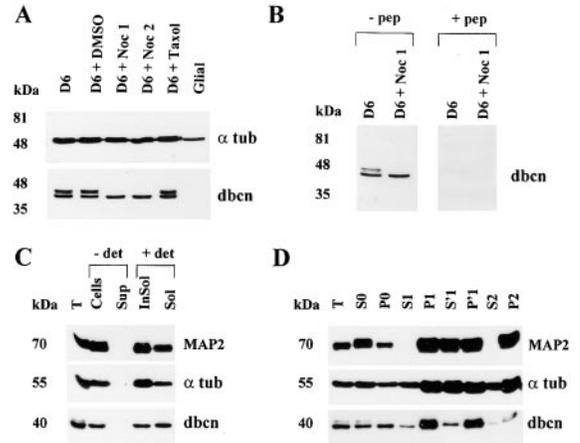

Figure 5. Association of Doublecortin with the Cytoskeleton

(A) Nonphosphorylated and phosphorylated Doublecortin (dbcn) was detected in neurons grown for 6 days (D6) and those treated with DMSO and taxol. Cells treated with two different amounts of nocodazole (D6 + Noc1, D6 + Noc2) retain only nonphosphorylated Doublecortin. A replicate Western blot was screened with an antibody directed against anti-α-tubulin. No Doublecortin expression was detected in glial cell extracts.
(B) Western blots were performed with the D6 and D6 + Noc1 samples, and the leftmost blot was screened with anti-Doublecortin pep antibodies as before, and the right blot with antibodies adsorbed with the synthetic peptide antigen.
(C) Detergent extraction of neuronal cells. Cells (T, total extract) were incubated in PEM ± 0.1% Triton X-100, and supernatants (Sup, Sol) and cell extracts (Cells, InSol) were analyzed for the presence of MAP2, α-tubulin, and Doublecortin. After extraction with detergent, Doublecortin was found in both soluble and insoluble fractions.
(D) Native Doublecortin is reversibly associated with MTs through cycles of polymerization and depolymerization and is mainly associated with MTs, which are stable at 0°C. Western blots (20 μg protein/lane) contain total mouse brain extracts (T), soluble cell components (S0), and insoluble cell components (P0). Both Doublecortin and MAP2 are found in both the soluble and insoluble fractions. The tubulin in the S0 fraction was polymerized to form MTs and sedimented, resulting in soluble (S1) and pellet (P1) fractions. Microtubules in P1 were incubated at 0°C for 1 hr and resedimented (S'1 and P'1). Note that the major proportion of Doublecortin cosediments with cold-stable MTs, whereas approximately 50% of MAP2 is found in the soluble fraction. The S'1 fraction was subjected to a further cycle of polymerization, followed by sedimentation (S2, P2). Doublecortin and MAP2 both associate with the newly formed MTs.

little or no effect of taxol on the Doublecortin staining pattern.

The results of these experiments were investigated by Western blot analysis. As shown in Figures 5A and 5B, three Doublecortin-specific bands are detected in control cells, whereas with nocodazole treatment the upper doublet is absent. These data hence suggest that the phosphorylated forms of Doublecortin are decreased in the presence of nocodazole. Neuronal cells were extracted with detergent in order to separate soluble proteins from the detergent-insoluble matrix, which consists of cytoskeletal polymers and associated proteins. Doublecortin, similar to MAP2, was found in both soluble and detergent-insoluble fractions (Figure 5C), suggesting that both free and cytoskeletal-associated forms exist. The proportions of insoluble and soluble α-tubulin after the detergent extraction were as expected (Audebert et al., 1993).

The association of Doublecortin with MTs was further tested. In sedimentation experiments using tubulin enriched from brain, native Doublecortin was found to cosediment with MTs in the same fraction as MAP2 (Figure 5D). With successive cycles of polymerization, Doublecortin was consistently found to sediment with newly formed microtubules. Interestingly, a depolymerization step at 0°C followed by sedimentation showed that the majority of Doublecortin remained associated with cold-stable microtubules whereas MAP2 was equally distributed between pellet and supernatant fractions (Figure 5D).

These results were further investigated using purified tubulin and a Doublecortin fusion protein. MTs were formed by polymerization with Taxol and incubated with GST–Doublecortin. Soluble proteins were separated from MTs by sedimentation. Using a constant amount of GST–Doublecortin and an increasing concentration of MTs resulted in the recruitment of Doublecortin to the pellet fraction. Treatment with 500 mM NaCl led to a release of Doublecortin into the supernatant fraction,
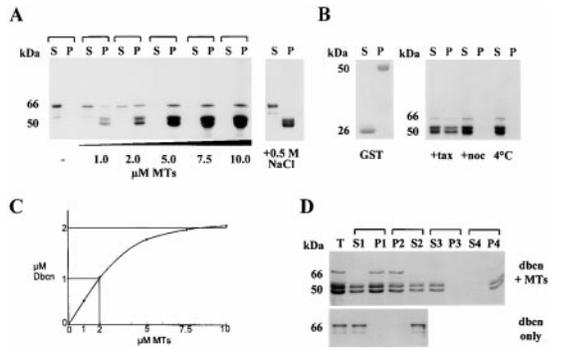
Figure 6. Doublecortin Interacts Directly with MTs and Remains Associated with Cold-Stable MTs In Vitro

(A) Affinity of Doublecortin for polymerized MTs at increasing tubulin concentrations. Coomassie blue-stained gels show that GST–Doublecortin (Mw, 66 kDa) cosediments with Taxol-stabilized MTs (P) assembled from purified tubulin. GST–Doublecortin is completely associated with the pellet fraction at high tubulin concentrations. In the presence of 500 mM NaCl, GST–Doublecortin dissociates from MTs.
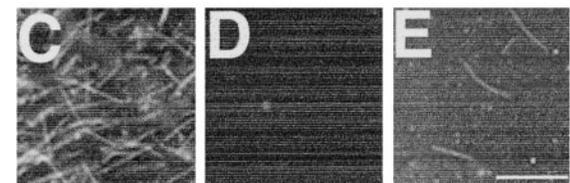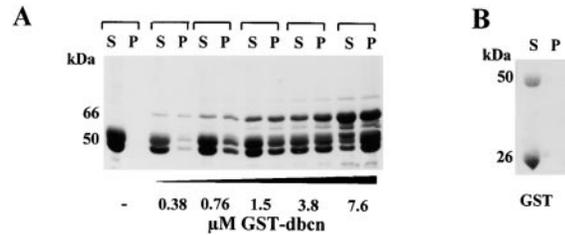
(B) Equivalent concentrations of GST control protein remain in the supernatant (S). The acrylamide concentration of the GST gel is higher (10%) than that of the GST–Doublecortin gel (8%) resulting in the differing mobilities of tubulin. The assembly of tubulin in the presence of GST–Doublecortin at either 37°C with taxol or nocodazole or at 4°C in their absence was performed. GST–Doublecortin is present in the supernatant fraction in the absence of MTs.

(C) The amount of GST–Doublecortin (Dbcn) bound to microtubules was quantified by densitometry and plotted to calculate the Kd. Half of the GST–Doublecortin (1 μM) is bound at 2 μM MTs.

(D) Doublecortin (dbcn) is associated with cold-stable MTs. Doublecortin was mixed with purified tubulin and allowed to polymerize (T). Sedimentation analysis shows that Doublecortin is associated with the formed MTs (P1). After depolymerization GST–Doublecortin is still found in the pellet fraction (P2) with the cold-stable MTs. GST–Doublecortin alone under the same conditions is soluble. With a further assembly cycle of the soluble tubulin (S2), the tubulin does not polymerize and remains in the supernatant (S3); however, with the addition of GST–Doublecortin, microtubules are re-formed (P4).

Figure 7. Doublecortin Induces MT Polymerization Shown by Sedimentation Studies and Fluorescence Microscopy

(A) Tubulin alone at 5 μM does not form MTs and, hence, remains in the supernatant fraction (S). With increasing concentrations of Doublecortin, MTs are formed as shown by increasing amounts of tubulin found in the pellet fraction.

(B) GST control protein does not cause polymerization of MTs.

(C–E) As observed by fluorescence microscopy, tubulin polymerizes at high concentrations (5 mg/ml) in the absence of Doublecortin (C), whereas at low concentrations (0.5 mg/ml) and in the presence of GST control, no MTs are formed (D). On addition of Doublecortin to low concentrations of tubulin (molar ratio, 1:5), MTs are formed (E). Scale bar, 5 μm.

whereas 5 mM GTP, GDP, ATP, and ADP had no effect (data not shown). GST control protein under the same conditions was exclusively present in the supernatant fraction (Figure 6B). Further controls using soluble purified tubulin were performed to demonstrate that the sedimented Doublecortin was associated with MTs. Purified tubulin was incubated either at 4°C or with taxol or nocodazole at 37°C in the presence of GST–Doublecortin (Figure 6B). In the presence of taxol, MTs are assembled and a proportion of Doublecortin is found in the pellet fraction. In the presence of nocodazole or at 4°C, no polymerization occurs and the tubulin and Doublecortin remain in the soluble fraction. Hence, Doublecortin cosediments specifically with MTs.

The data presented in Figure 6A were quantified by densitometry and plotted (Figure 6C), to estimate the binding affinity (Kd), determined as the quantity of MTs required to bind half of the available protein (Butner and Kirschner, 1991). At a concentration of 2 μM MTs, 50% of the Doublecortin present was bound (Figures 6A and 6C). We next tested the in vitro association of GST–Doublecortin and MTs through cycles of polymerization and depolymerization (Figure 6D). After the first polymerization cycle, Doublecortin was found to be associated with the MTs, as expected. The sedimented material

was depolymerized at 0°C for 30 min and recentrifuged. A large amount of Doublecortin was found to be still associated with a proportion of cold-stable MTs, mimicking results observed with native Doublecortin. GST–Doublecortin alone under the same conditions was present in the soluble fraction. It was not possible to re-form MTs using the S3 tubulin fraction alone, suggesting that the concentration was too low. A further polymerization step, however, with added GST–Doublecortin led to MT assembly (P4). These latter data suggest that Doublecortin reduces the critical concentration of tubulin required for MT assembly.

The effect of GST–Doublecortin on the polymerization of MTs was further tested. As shown by sedimentation, at low concentrations (5 μM) soluble tubulin alone does not polymerize; however, in the presence of GST–Doublecortin, increasing quantities of MTs were sedimented (Figure 7A). The GST control protein had no effect on tubulin polymerization (Figure 7B). Hence, Doublecortin reduces the critical concentration required for MT formation. Similar results were observed by microscopy using rhodamine-labeled tubulin (Figures 7C–7E). Immunofluorescence studies further showed a direct colocalization between MTs and GST–Doublecortin (data not shown). Taken together, these data indicate that Doublecortin binds to MTs in vitro with an affinity similar to other microtubule-associated proteins (Gustke et al., 1994). In addition, Doublecortin is capable of inducing the polymerization of purified tubulin, and its association with cold-stable MTs suggests that it may play a role in MT stabilization.

Discussion

We have shown that Doublecortin is widely expressed in the CNS and at least in some parts of the PNS. In mouse, its expression begins at embryonic day 10.5/11 and widespread expression continues until neonatal stages. The start of Doublecortin expression therefore corresponds to the early stages of neurogenesis, when neocortical neurons destined for the developing cortex are generated and begin their migration process (reviewed by Caviness et al., 1997). This process takes place during mouse embryonic day 11 and embryonic day 17. Our data show that Doublecortin expression is not limited to this period and continues in cells that have completed their migration. Indeed, in the developing cortex of both mouse and rat, Doublecortin was found to be abundantly expressed in the cells of the preplate and cortical plate. A strong axonal labeling in the intermediate zone was observed showing that Doublecortin is expressed in differentiating neurons.

Previously, it has been shown that tangentially migrating neurons exist within the proliferative layers of the developing cortex (O'Rourke et al., 1992; Menezes and Luskin, 1994; O'Rourke et al., 1995). Doublecortin was found to be expressed in ventricular zone neurons of tangential orientation, which coexpressed β III tubulin (Lee et al., 1990). These cells showed a characteristic neuronal morphology, with long leading processes suggesting they were actively migrating. It is still unclear if radially migrating neurons in the intermediate zone also express Doublecortin, because axonal tracts mask their signal. Thus, the question still remains as to whether Doublecortin is critical for the migration of all types of neuron, including the limited numbers of migrating cells in the adult brain (Doetsch and Alvarez-Buylla, 1996). Further studies including a comparison of expression in other species are required to fully answer these questions. The clear expression of Doublecortin in neurons that have apparently reached their final destination might suggest that axonal pathfinding errors are the primary defect in X-linked lissencephaly and SCLH, challenging the current hypothesis that these are neuronal migration disorders. It is also interesting to note that the process of corticogenesis is specifically disrupted in affected individuals, contrasting with the wide expression of Doublecortin in the developing nervous system. It is very likely that Doublecortin is critical for cortical development but perhaps its function can be replaced by homologous proteins in other regions. Indeed, at least one homologous gene has been identified (des Portes et al., 1998a; Gleeson et al., 1998).

Developing neurons in culture extend neuritic processes that take on the characteristics of axons and dendrites. Growth cones can be observed at the tips of some growing neurites, and cytoskeletal components, such as the heterogeneous forms of tubulin have been shown to be regulated with a temporal pattern mimicking that observed during development in vivo (Audebert et al., 1994). The expression of Doublecortin in cultured neurons is concentrated in the distal regions of neurites. Similar distribution patterns have been recently reported for a MT motor protein, Eg5, in cultures of hippocampal neurons (Ferhat et al., 1998). Interestingly, MAP2 expression was low or absent from the regions that stained intensely for Doublecortin, suggesting that these two proteins have nonredundant roles. The significance of these staining patterns with respect to neuronal migration and differentiation is unclear. It is difficult to extrapolate from results obtained in maturing neurons in culture, to neurons that are actively migrating or differentiating in vivo. Unlike neurite outgrowth, neuronal migration involves an extension of a leading process toward the target destination followed by the translocation of the nucleus and other cytoplasmic organelles (Komuro and Rakic, 1995). The leading process exhibits rapid extensions and retractions during cell locomotion (Rivas and Hatten, 1995), whereas axon extension results in net lengthening. In growing axons, MTs are distributed into distinct compartments: stabilized, bundled MTs are found along their whole length (reviewed by Gordon-Weeks, 1991), whereas in the growth cone, single MTs and unpolymerized tubulin provide a more dynamic component allowing growth cone flexibility and its ability to respond to directional information (reviewed by Tanaka and Sabry, 1995). Several stabilization processes presumably occur in the transition region of the neurite shaft-growth cone boundaries where Doublecortin is enriched in neurons in culture.

We have performed experiments indicating that Doublecortin is associated with MTs and cosediments in the same fraction as MAP2. Experiments using phosphocellulose purified tubulin and a purified Doublecortin fusion protein demonstrate a direct interaction. The affinity of Doublecortin for MTs is comparable with that of conventional MAPs (Gustke et al., 1994), although tubulin-binding motifs found in MAP2 and tau are not evident in the Doublecortin sequence. Conditions of high ionic strength lead to the dissociation of Doublecortin from the MTs, as has previously been determined with other MAPs (Vallee, 1982). Doublecortin was further shown to induce polymerization of MTs in vitro in both microscopical and sedimentation studies. These combined data suggest that Doublecortin is a novel MT-associated protein. However, our preliminary data suggest that Doublecortin exhibits a different behavior to MAP2 and tau (reviewed by Goedert et al., 1991). Doublecortin is associated with stable MTs that are resistant to cold treatment. In this respect, Doublecortin is more similar to the STOP proteins, which are MAPs involved in MT stabilization (Guillard et al., 1998).

A role of Doublecortin as a MAP that induces polymerization and enhances stabilization is in agreement with a protein required for either neuronal migration or differentiation. Induction of polymerization in the migrating cell may contribute to the forces required for locomotion. Although MAP2 and tau have functions in both the developing and adult brain (reviewed by Tucker, 1990), to our knowledge, their specific role in neuronal migration has not been documented. Doublecortin may hence be a MAP specifically required in neuronal migration. In addition, unlike the STOP proteins, MAP2 and tau do not confer cold-stability to MTs (Baas et al., 1994). Doublecortin may thus be a specific neuronal MAP regulating stabilization processes in certain neuronal cells during development.

Altogether, our data provide new insights into the molecular and cellular mechanisms underlying the severe

cortical malformations resulting from a deficit of Doublecortin. It appears from our study that Doublecortin is not expressed in proliferating cells but is present in young migrating and differentiating neurons. An association with MTs could equally suggest a role in neuronal locomotion or a role in morphogenesis, since MTs are critical for both processes. It is interesting to point out that LIS1 has recently been shown to influence MT dynamics (Sapir et al., 1997) and that *Lis1* knockout mice exhibit abnormal neuronal migration (Hirotsune et al., 1998). Further studies including animal models, aiming to dissect the interaction between Doublecortin, the cytoskeleton, and other regulating or interacting proteins, are required to gain a better understanding of the regulation of MT dynamics and its involvement in neuronal migration and differentiation.

Experimental Procedures

Antibodies
Synthetic peptides corresponding to Doublecortin amino acids 1–10, 287–296, and 350–360 (GenEmbl sequence AJ003112) were used to produce polyclonal antibodies (anti-Doublecortin pep). A BamHI N-terminal GST fusion protein was produced in pGEX-4T1, containing the first 110 amino acids (N-term), and was also used to produce polyclonal antibodies. A full-length Doublecortin fusion protein was similarly prepared in pGEX-4T1; this and GST control protein were column purified using glutathionine sepharose 4B (Pharmacia Biotech, Orsay, France).

For Western blot analysis, anti-Doublecortin pep antibodies were used at 1:1000 and anti-N-term at 1:8000. GT335, a mAb specific for glutamylated tubulin (Wolff et al., 1992), was used at 1:10,000. A monoclonal antibody directed against α-tubulin (Amersham, N. 356 [Les Ulis, France]) was used at 1:10,000. Anti-MAP2 (Sigma-Aldrich, M-4403 [Saint Quentin Fallavier, France]) was used at 1:4000 and recognizes MAP2a, MAP2b, and MAP2c; the latter (70 kDa) is the major form expressed in the developing brain.

Cell Cultures
Primary neuronal cultures were prepared from fetal mouse brain at 15 days of gestation as previously described (Berwald-Netter et al., 1981). In some experiments, neurons were treated for 4 hr with taxol (10 μg/ml) or nocodazole (3.5 or 8 μM). DMSO, which was used to solubilize the drugs, was added in controls (1/1000 vol/vol). Glial cultures containing > 95% astrocytes and devoid of neurons were prepared according to Nowak et al. (1987) from newborn mouse cerebral hemispheres and used as secondary cultures. The detergent extraction of neuronal cells was performed as described previously (Audebert et al., 1993).

Cell and Tissue Extracts
Cell and tissue extracts were prepared according to conventional methods. Samples were loaded on 11% SDS-PAGE separation gels, and immunodetection was performed using an ECL detection kit (Amersham) following manufacturer's instructions.

Phosphatase Treatment of Tissue Extracts
Frozen neonatal mouse brain tissue (100 mg) was finely ground in liquid nitrogen and taken up in 1 ml of 50 mM Tris-HCl (pH 7.5), 1 mM MgCl₂, with protease inhibitors (Complete [Boehringer Mannheim Biochemicals, Mannheim, Germany]). The resuspension was centrifuged at 15,500 g at 4°C for 1 hr and 50 μl aliquots of the supernatant were diluted 1:2 in a phosphatase assay (detailed in figure legends). Each sample (25 μl) was subjected to Western blot analysis.

Immunocytochemical Staining
Neurons grown on coverslips were fixed in 2% paraformaldehyde, 0.1% picric acid in PBS for 1 hr at room temperature. After four washes in PBS, fixed cells were processed for immunocytochemical staining and incubated overnight at 4°C with the primary antibodies

(anti-Doublecortin pep, 1:300; anti-N-term, 1:300–1:4000; anti-actin, 1:200; anti-MAP2, 1:500; and anti-α-tubulin, 1:1000). After three washes, cells were incubated for 1 hr at room temperature with affinity-purified secondary antibodies (FITC conjugated goat anti-rabbit Ig [Biosys, Compiegne, France]; Texas Red–conjugated goat anti-mouse Ig [Jackson ImmunoResearch Laboratories, West Grove, PA]). After three washes, cells were finally rinsed in TBS, mounted in Mowiol, and examined using a Zeiss microscope equipped with epifluorescence illumination.

In Situ Hybridizations and Peroxidase Immunodetection in Mouse Embryonic Sections
In vitro transcription was performed using a doublecortin clone containing sequences of the 5′ UTR exons 1A and 1B (des Portes et al., 1998a) and upstream sequences. For all experiments, sense and antisense probes were generated in parallel in order to assess specificity of the signal. Mouse embryos were fixed in 2%–4% paraformaldehyde, cryoprotected with 30% sucrose in phosphate buffer, frozen with isopenthan, and stored at −20°C until sectioning. Briefly, hybridization of sections (15–20 μm thick) with $α^{35}S$-labeled RNA probes was carried out in a 50% formamide solution at 58°C. Sections were washed in 50% formamide and then successively stringent SSC wash solutions, with a final wash at 0.1 × SSC at 60°C. Slides were dipped in diluted Kodak NTB2 emulsion and exposed for 5 to 15 days. Emulsions were developed and sections counterstained with toluidine blue, mounted in Eukitt, and examined under light microscopy. Immunodetections were performed using a Vectastain kit (Vector Laboratories, CA) following manufacturer's instructions. In all experiments, results with preimmune sera were compared with anti-Doublecortin antibodies, and endogeneous peroxidase was assessed in the absence of antibodies.

Rat Embryonic Brain Histochemistry
Sections (20 μm) from Long Evans (Sprague Dawley) rats (vaginal plug is counted as embryonic day 1) were permeabilized and blocked overnight in a humidified chamber with blocking buffer: 15% normal goat serum/1 mg/ml BSA/0.5% triton X-100 in phosphate buffered saline (pH 7.0). Preimmune, anti-Doublecortin pep, and anti-N-term sera were all used at a 1:500 dilution in blocking buffer at room temperature for 2–12 hr. Anti-β III tubulin (TuJ1) monoclonal antibodies (BAbCO, Richmond, CA) were also used at 1:500. Secondary antibodies (Texas Red goat anti-rabbit and Cy-2 donkey anti-mouse [Jackson Immunoresearch, PA]) were used at 1:200 dilution in blocking buffer for 45 min, at room temperature. DNA was visualized in some cases using 1 mM Syto-11 (Molecular Probes, Eugene, OR) included with the secondary antibodies. Slides were mounted in Fluoromount-G (Southern Biotechnology Associates, Birmingham, AL) and imaged using a MRC-600 confocal scanning microscope (BioRad, Richmond, CA). Images were merged using Adobe Photoshop 4.0.

Purification of Tubulin and Sedimentation Experiments
The temperature-dependent polmerization-depolymerization experiment was performed as follows: a brain fraction enriched in tubulin was prepared from 2-day-old mice by homogenization in MEM buffer (50 mM MES [pH 6.8], 2 mM EGTA, 2 mM MgCl₂) with protease inhibitors and ultracentrifugation (150,000 g at 4°C for 1 hr). Soluble tubulin (S0) was incubated in the presence of 1 mM GTP and 25% glycerol for 40 min at 37°C to form MTs that were sedimented (150,000 g) for 60 min at 30°C. The resulting pellet (P1) was depolymerized for 60 min at 0°C and gently homogenized. Sedimentation of the insoluble (P′1) from soluble components (S′1) was performed. Soluble tubulin (S′1) was repolymerized as before giving rise to P2 and S2 fractions.

Purified tubulin was prepared from a 100,000 g supernatant of adult mouse brain by two cycles of assembly-disassembly and further purified by phosphocellulose (PC) column chromatography (P11 [Whatman, Maidstone, United Kingdom]) in MEM buffer containing 1 mM GTP and a mixture of protease inhibitors. This tubulin was used for assembly and control experiments. MTs were formed by taxol hyperpolymerization of a MAP-depleted tubulin fraction. Increasing amounts of MTs (0–10 μM) were added to a constant amount of precleared GST–Doublecortin (2 μM). MTs and bound

Doublecortin were separated from soluble forms by ultracentrifugation through a 60% glycerol cushion (10 min at 30,000 g on Airfuge [Beckman, Palo Alto, CA]). Samples were analyzed by Coomassie blue staining, and quantities of bound Doublecortin assessed by densitometry (Multi-Analyst [BioRad, Hercules, CA]). Further treatments of the Doublecortin associated MTs included the addition of NaCl (final concentration, 500 mM), GTP, GDP, ATP, or ADP nucleotides (each 5 mM).

To test the effect of Doublecortin on polymerization, PC-purified tubulin (5 μM) was polymerized in the presence of 1 mM GTP, and with increasing concentrations of GST–Doublecortin (0–7.6 μM) for 20 min at 37°C. To test the association of Doublecortin through cycles of polymerization and depolymerization, MTs (7.5 μM) were assembled under the same conditions in the presence of GST–Doublecortin (2 μM), the sedimented MTs were depolymerized by incubation at 0°C for 30 min and recentrifuged. The supernatant (S2) was repolymerized alone and sedimented. The soluble fraction (S3) was further polymerized in the presence of 0.75 μM GST–Doublecortin. Samples were analyzed by Coomassie blue staining.

Rhodamine-Tubulin Microscopy Experiments

Tubulin and rhodamine-tubulin were purchased from Molecular Probes (Eugene, OR) and mixed at a ratio of 4:1 unlabeled to labeled at a final concentration of either 5 mg/ml (positive control), or 0.55 mg/ml when testing the effect of the added fusion protein. Reactions were performed in 1× GPEM buffer (1 mM GTP, 80 mM PIPES [pH 7.0], 1 mM EGTA, 5 mM MgCl$_2$) with 10% glycerol at either 37°C for 30 min (positive control) or 26°C. Either purified GST–Doublecortin or GST control were mixed with tubulin at a 1:5 molar ratio. Reactions were diluted in 1× GPEM with 60% glycerol, spread on microscope slides, and observed using fluorescence microscopy.

References

Audebert, S., Desbruyères, E., Gruszczynski, C., Koulakoff, A., Gros, F., Denoulet, P., and Eddé, B. (1993). Reversible polyglutamylation of α- and β-tubulin and microtubule dynamics in mouse brain neurons. Mol. Biol. Cell 4, 615–626.

Audebert, S., Koulakoff, A., Berwald-Netter, Y., Gros, F., Denoulet, P., and Eddé, B. (1994). Developmental regulation of polyglutamylated α- and β-tubulin in mouse brain neurons. J. Cell Sci. 107, 2313–2322.

Baas, P.W., Pienkowski, T.P., Cimbalnik, K.A., Toyama, K., Bakalis, S., Ahmad, F.J., and Kosik, K.S. (1994). Tau confers drug stability but not cold stability to microtubules in living cells. J. Cell Sci. 107, 135–143.

Bernhardt, R., and Matus, A. (1984). Light and electron microscopic studies of the distribution of microtubule-associated protein 2 in rat brain: a difference between dendritic and axonal cytoskeletons. J. Comp. Neurol. 226, 203–231.

Berwald-Netter, Y., Martin-Moutot, N., Koulakoff, A., and Couraud, F. (1981). Na$^+$-channel-associated scorpion toxin receptor sites as probes for neuronal evolution in vivo and in vitro. Proc. Natl. Acad. Sci. USA 78, 1245–1249.

Butner, K.A., and Kirschner, M.W. (1991). Tau protein binds to microtubules through a flexible array of distributed weak sites. J. Cell Biol. 115, 717–730.

Caviness, V.S., Jr., Takahashi, T., and Nowakowski, R.S. (1997). Cell proliferation in cortical development. In Normal and Abnormal Development of the Cortex. A.M. Galaburda and Y. Christen, eds. (Berlin/Heidelberg: Springer-Verlag), pp. 1–24.

Chae, T., Kwon, Y.T., Bronson, R., Dikkes, P., Li, E., and Tsai, L.H. (1997). Mice lacking p35, a neuronal specific activator of Cdk5, display cortical lamination defects, seizures, and adult lethality. Neuron 18, 29–42.

D'Arcangelo, G., Miao, G.G., Chen, S.C, Soares, H.D., Morgan, J.I., and Curran, T. (1995). A protein related to extracellular matrix proteins deleted in the mouse mutant reeler. Nature 374, 719–723.

des Portes, V., Pinard, J.M., Billuart, P., Vinet, M.C., Koulakoff, A., Carrié, A., Gelot, A., Dupuis, E., Motte, J., Berwald-Netter, Y., Catala, C., Kahn, A., Beldjord, C., and Chelly, J. (1998a). Identification of a novel CNS gene required for neuronal migration and involved in X-linked subcortical laminar heterotopia and lissencephaly syndrome. Cell 92, 51–61.

des Portes, V., Francis, F., Pinard, J.-M., Desguerre, I., Moutard, M.-L., Snoeck, I., Meiners, L.C., Capron, F., Cusmai, R., Ricci, S., Motte, J., Echenne, B., Ponsot, G., Dulac, O., Chelly, J., and Beldjord, C. (1998b). Doublecortin is the major gene causing X-linked Subcortical Laminar Heterotopia (SCLH). Hum. Mol. Gen. 7, 1063–1070.

Dobyns, W.B., Curry, C.J.R., Hoyme, H.E., Turlington, L., and Ledbetter, D.H. (1991). Clinical and molecular diagnosis of Miller-Dieker syndrome. Am. J. Hum. Genet. 48, 584–594.

Doetsch, F., and Alvarez-Buylla, A. (1996). Network of tangential pathways for neuronal migration in adult mammalian brain. Proc. Natl. Acad. Sci. USA 93, 14895–14900.

Ferhat, L., Cook, C., Chauviere, M., Harper, M., Kress, M., Lyons, G.E., and Baas, P.W. (1998). Expression of the mitotic motor protein Eg5 in postmitotic neurons: implications for neuronal development. J. Neurosci. 18, 7822–7835.

Frantz, G.D., and McConnell, S.K. (1996). Restriction of late cerebral cortical progenitors to an upper-layer fate. Neuron 17, 55–61.

Gleeson, J.G., Allen, K.M., Fox, J.W., Lamperti, E.D., Berkovic, S., Scheffer, I., Cooper, E.C., Dobyns, W.B., Minnerath, S.R., Ross, M.E., and Walsh, C.A. (1998). doublecortin, a brain-specific gene mutated in human X-linked lissencephaly and double cortex syndrome, encodes a putative signaling. Cell 92, 63–72.

Goedert, M., Crowther, R.A., and Garner, C.C. (1991). Molecular characterization of microtubule-associated proteins Tau and MAP2. Trends Neurosci. 14, 193–199.

Gordon-Weeks, P.R. (1991). Growth cones: the mechanism of neurite advance. BioEssays 13, 235–239.

Guillard, L., Bosc, C., Fourest-Lieuvin, A., Denarier, E., Pirollet, F., Lafanechère, L., and Job, D. (1998). STOP proteins are responsible for the high degree of microtubule stabilization observed in neuronal cells. J. Cell Biol. 142, 167–179.

Gustke, N., Trinczek, B., Biernat, J., Mandelkow, E.-M., and Mandelkow, E. (1994). Domains ot tau protein and interactions with microtubules. Biochemistry 33, 9511–9522.

Harding, B. (1996). Gray matter heterotopia. In Dysplasias of Cerebral Cortex and Epilepsy. R. Guerrini, F. Andermann, R. Canapicchi, J. Roger, B. Zilfkin, and P. Pfanner, eds. (Philadelphia/New York: Lippincott-Raven), pp. 81–88.

Hattori, M., Adachi, H., Tsujimoto, M., Arai, N., and Inoue, K. (1994). Miller Dieker lissencephaly gene encodes a subunit of brain platelet-activating factor acetylhydrolase. Nature 370, 216–218.

Hirotsune, S., Takahara, T., Sasaki, N., Hirose, K., Yoshiki, A., Ohashi, T., Kusakabe, M., Murakami, Y., Muramatsu, M., Watanabe, S., et al. (1995). The reeler gene encodes a protein with an EGF-like motif expressed by pioneer neurons. Nat. Genet. 10, 77–83.

Hirotsune, S., Fleck, M.W., Gambello, M.J., Bix, G.J., Chen, A., Clark, G.D., Ledbetter, D.H., McBain, C.J., and Wynshaw-Boris, A. (1998). Graded reduction of Pafah1b1 (Lis1) activity results in neuronal migration defects and early embryonic lethality. Nat. Genet. 19, 333–339.

Howell, B.W., Hawkes, R., Soriano, P., Cooper, J.A. (1997). Neuronal position in the developing brain is regulated by mouse disabled-1. Nature 389, 733–737.

Komuro, H., and Rakic, P. (1995). Dynamics of granule cell migration: a confocal microscopic study in acute cerebellar slice preparations. J. Neurosci. *15*, 1110–1120.

Lee, M.K., Tuttle, J.B., Rebhun, L.I., Cleveland, D.W., and Frankfurter, A. (1990). The expression and posttranslational modification of a neuron-specific β-tubulin isotype during chick embryogenesis. Cell Motil. Cytoskel. *17*, 118–132.

Lois, C., Garcia-Verdugo, J.-M., and Alvarez-Buylla, A. (1996). Chain migration of neuronal precursors. Science *271*, 978–981.

Luskin, M.B. (1993). Restricted proliferation and migration of postnatally generated neurons derived from the forebrain subventricular zone. Neuron *11*, 173–189.

Luskin, M.B., Pearlman, A.L., and Sanes, J.R. (1988). Cell lineage in the cerebral cortex of the mouse studied in vivo and in vitro with a recombinant retrovirus. Neuron *1*, 635–647.

McConnell, S.K. (1995). Constructing the cerebral cortex: neurogenesis and fate determination. Neuron *15*, 761–768.

Menezes, J.R.L., and Luskin, M.B. (1994). Expression of neuron-specific tubulin defines a novel population in the proliferative layers of the developing telencephalon. J. Neurosci. *14*, 5399–5416.

Nikolic, M., Chou, M.M., Lu, W., Mayer, B.J., and Tsai, L.-H. (1998). The p35/Cdk5 kinase is a neuron-specific Rac effector that inhibitis Pak1 activity. Nature *395*, 194–198.

Nowak, L., Ascher, P., and Berwald-Netter, Y. (1987). Ionic channels in mouse astrocytes in culture. J. Neurosci. *7*, 101–109.

Ohshima, T., Ward, J.M., Huh, C.G., Longenecker, G., Veeranna. Pant, H.C., Brady, R.O., Martin, L.J., and Kulkarni, A.B. (1996). Targeted disruption of the cyclin-dependent kinase 5 gene results in abnormal corticogenesis, neuronal pathology and perinatal death. Proc. Natl. Acad. Sci. USA *93*, 11173–11178.

O'Rourke, N.A., Dailey, M.E., Smith, S.J., and McConnell, S.K. (1992). Diverse migratory pathways in the developing cerebral cortex. Science *258*, 299–302.

O'Rourke, N.A., Sullivan, D.P., Kaznowski, C.E., Jacobs, A.A., and McConnell, S.K. (1995). Tangential migration of neurons in the developing cerebral cortex. Development *121*, 2165–2176.

Pearlman, A.L., Faust, P.L., Hatten, M.E., and Brunstrom, J.E. (1998). New directions for neuronal migration. Curr. Opin. Neurobiol. *8*, 45–54.

Pinard, J.-M., Motte, J., Chiron, C., Brian, R., Andermann, E., and Dulac, O. (1994). Subcortical laminar heterotopia and lissencephaly in two families: a single X linked dominant gene. J. Neurol. Neurosurg. Psychiatry *57*, 914–920.

Rakic, P. (1971). Neuron–glia relationship during granule cell migration in developing cerebellar cortex. A Golgi and electron microscope study in Macacus rhesus. J. Comp. Neurol. *141*, 283–312.

Rakic, P., Knyihar-Csillik, E., and Csillik, B. (1996). Polarity of microtubule assemblies during neuronal cell migration. Proc. Natl. Acad. Sci. USA *93*, 9218–9222.

Reiner, O., Carrozzo, R., Shen, Y., Wehnert, M., Faustinella, F., Dobyns, W.B., Caskey, C.T., and Ledbetter, D.H. (1993). Isolation of a Miller-Dieker lissencephaly gene containing G protein β-subunit-like repeats. Nature *364*, 717–721.

Rivas, R.J., and Hatten, M.E. (1995). Motility and cytoskeletal organization of migrating cerebellar granule neurons. J. Neurosci. *15*, 981–989.

Sapir, T., Elbaum, M., and Reiner, O. (1997). The lissencephaly 1 (LIS1) gene product interacts with tubulin and reduces microtubule catastrophe events. EMBO J. *16*, 101–108.

Sheldon, M., Rice, D.S., D'Arcangelo, G., Yoneshima, H., Nakajima, K., Mikoshiba, K., Howell, B.W., Cooper, J.A., Goldowitz, D., and Curran, T. (1997). *Scrambler* and *yotari* disrupt the disabled gene and produce a reeler-like phenotype in mice. Nature *389*, 730–733.

Tan, S.-S., and Breen, S.J. (1993). Radial mosaicism and tangential cell dispersion both contribute to mouse neocortical development. Nature *362*, 638–640.

Tanaka, E., and Sabry, J. (1995). Making the connection: cytoskeletal rearrangements during growth cone guidance. Cell *83*, 171–176.

Tucker, R.P. (1990). The roles of microtubule-associated proteins in brain morphogenesis: a review. Brain Res. Brain Res. Rev. *15*, 101–120.

Vallee, R.B. (1982). A taxol-dependent procedure for the isolation of microtubules and microtubule-associated proteins (MAPs). J. Cell Biol. *92*, 435–442.

Ware, M.L., Fox, J.W., Gonzalez, J.L., Davis, N.M., Lambert de Rouvroit, C., Russo, C.J., Chua, S.C., Jr., Goffinet, A.M., and Walsh, C.A. (1997). Aberrant splicing of a mouse disabled homolog, mdab1, in the scrambler mouse. Neuron *19*, 1–20.

Wolff, A., Néchaud, B.D., Chillet, D., Mararguil, H., Desbruyères, E., Audebert, S., Eddé, B., Gros, F., and Denoulet, P. (1992). Distribution of glutamylated α- and β-tubulin in mouse tissues using a specific monoclonal antibody, GT335. Eur. J. Cell. Biol. *59*, 425–432.